Poster Reprint

ASMS 2025
Poster number TP 059

Dynamically Adjusted Instrument Settling Delay Prior to Data Acquisition

Haopeng Wang, Behrooz Zekavat, Laura L Pollum, Huy Nguyen, Patrick M Batoon

Agilent Technologies Inc., Santa Clara, CA

Introduction

Quadrupole mass spectrometers coupled to separation techniques are widely used for targeted analyses of complex samples with fast acquisition speeds. To maintain reliable instrument performance independent of acquisition speed, it is important to use appropriate inter-measurement delays and ensure timely settling of instrument electronics and ion signal without sacrificing duty cycle.

To achieve this goal, it is critical to select “optimal” delay times at which ion flux has reached to a stable level at the detector. The “optimum” delay times should be adjusted dynamically according to the acquisition parameters before and after the transition.

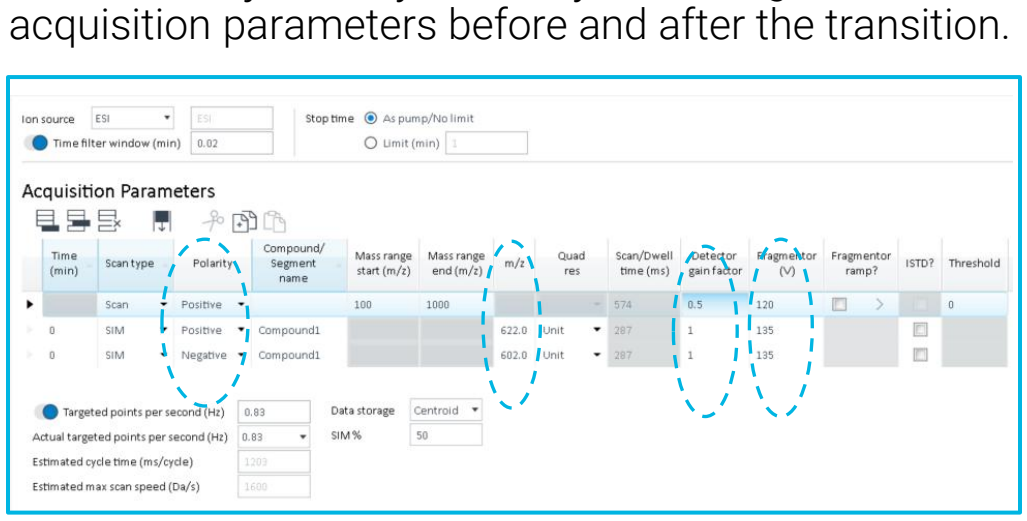

Figure 1. Example of acquisition method editor for LC/SQ mass spectrometer.

Typical acquisition parameters for single quadrupole instruments are shown in Figure 1. Parameters which could change between two consecutive measurements include 1) *m/z* setting on the quadrupole mass filter (associated with RF and DC voltages applied on quadrupole), 2) fragmentor voltage, 3) Detector gain factor, and 4) ion polarity.

Here, we present results from ion signal settling time measurements after selected jumps of acquisition parameters. All experiments were done on Agilent Pro iQ series LC/SQ mass spectrometers. Figure 2 shows the schematic view of the ion optics. It is important to note that the ion signal settling is affected by both the settling of electronics and ion transit into the detector.

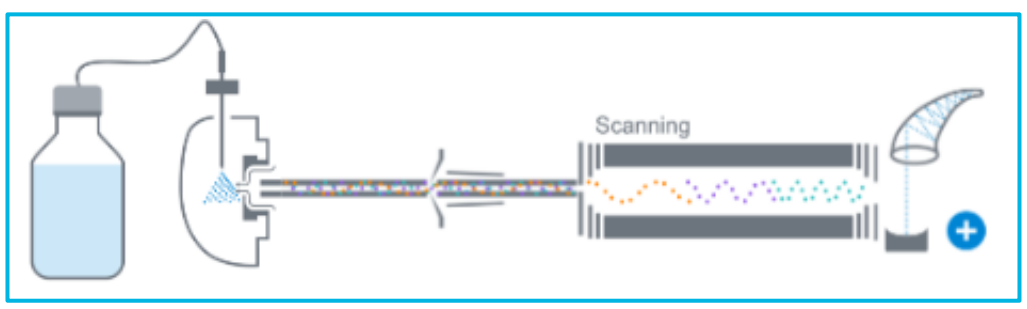

Figure 2. Schematic of LC/SQ mass spectrometer

Experimental

Ion signal measurements with capture mode.

Ion signal measurements were performed on Agilent Pro iQ series LC/SQ mass spectrometers with electrospray ionization source and Agilent ESI-L tuning standard.

Ion abundance data was acquired in capture mode using built-in Python scripts. At time 0, one of the acquisition parameters was changed to mimic the transition between two measurements. The ion signal was continuously monitored every 16 µs and was plotted against the time since the parameter changed. The time-abundance data were processed by Python to provide real-time feedbacks and were saved into *.csv format for post-processing. Data files were processed in MATLAB for settling time extraction, curve fitting and plotting purposes. Abundance data were acquired by changing 1) *m/z*, 2) fragmentor voltage, 3) detector gain factor and 4) ion polarity.

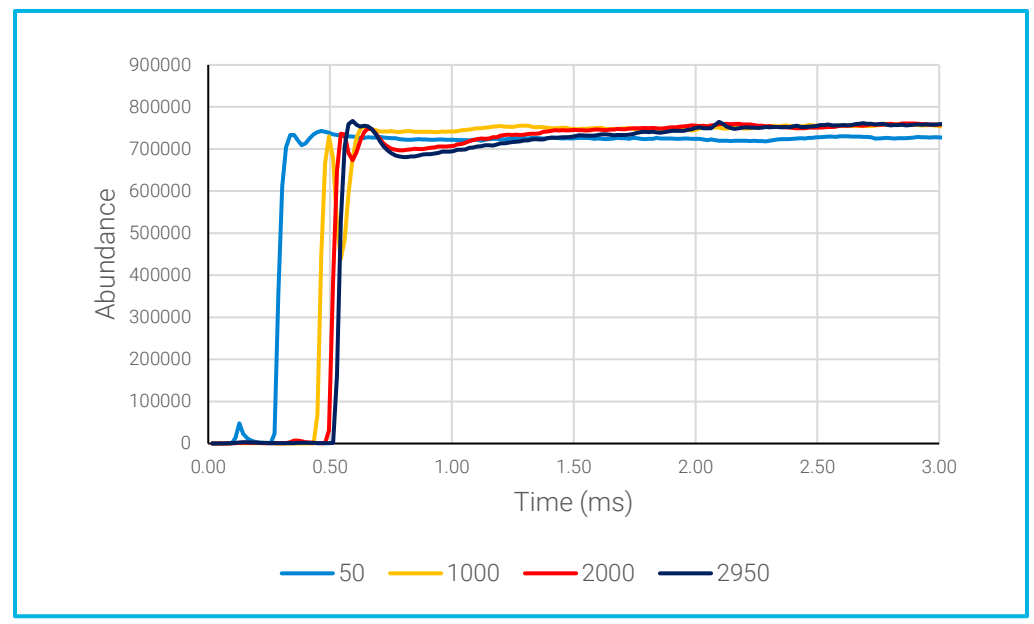

Figure 3. Ion abundance data in capture mode with *m/z* jump from multiple settings to 113.

Implementation and validation of multi-dimensional inter-measurement delay coefficients.

With experimental ion settling data, multiple correlations between acquisition parameters and settling time were established. Curve fitting generated polynomial coefficients for simple implementation into instrument control firmware (or embedded software).

A mixture of Agilent pesticides (submix 5 and 7) and HSA peptides was analyzed on Agilent Ultivo LC/TQ instrument. To validate the predicted inter-measurement delay, abundance data were collected at various dwell time for all transitions.

Results and Discussion

Ion signal settling time is characterized against changes in mass axis setting (*m/z*), fragmentor voltage, detector gain factors and ion polarity.

Mass axis delay

To determine the ion signal settling for various ions, capture mode data were collected by jumping *m/z* from various starting point to the *m/z* corresponding to each calibrant ion. Figure 4 shows the settling time as function of initial and final mass.

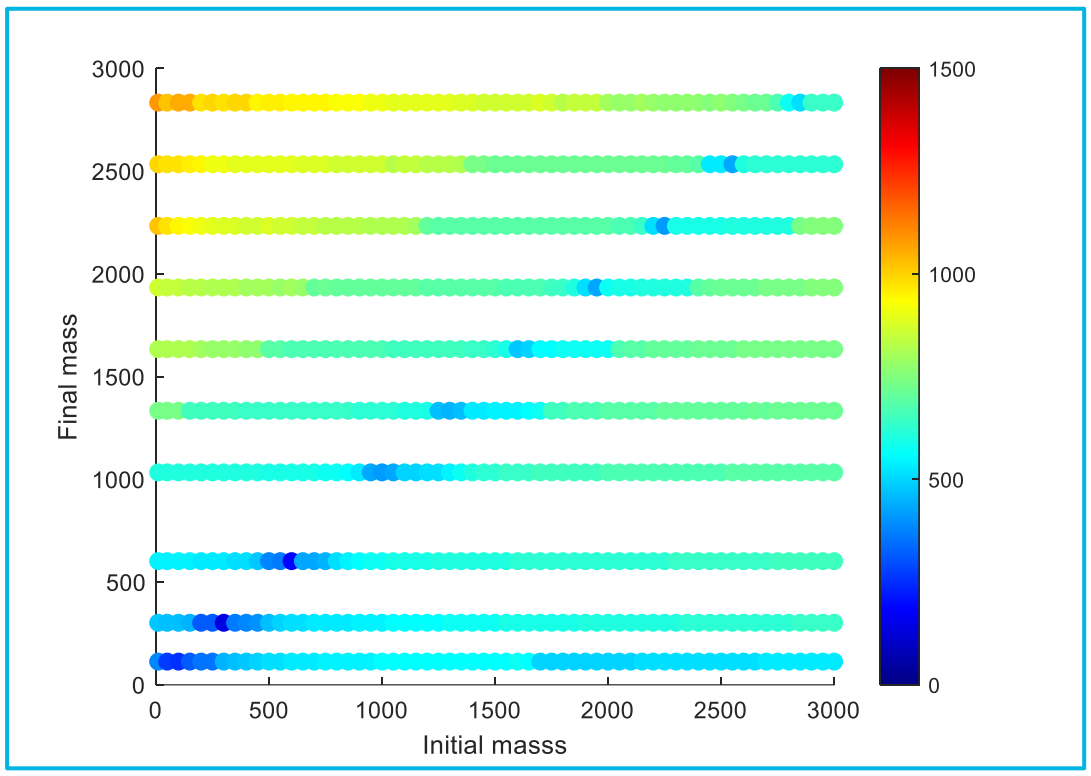

Figure 4. Ion abundance settling time vs initial and final mass. Settling time in µs is indicated by the color map.

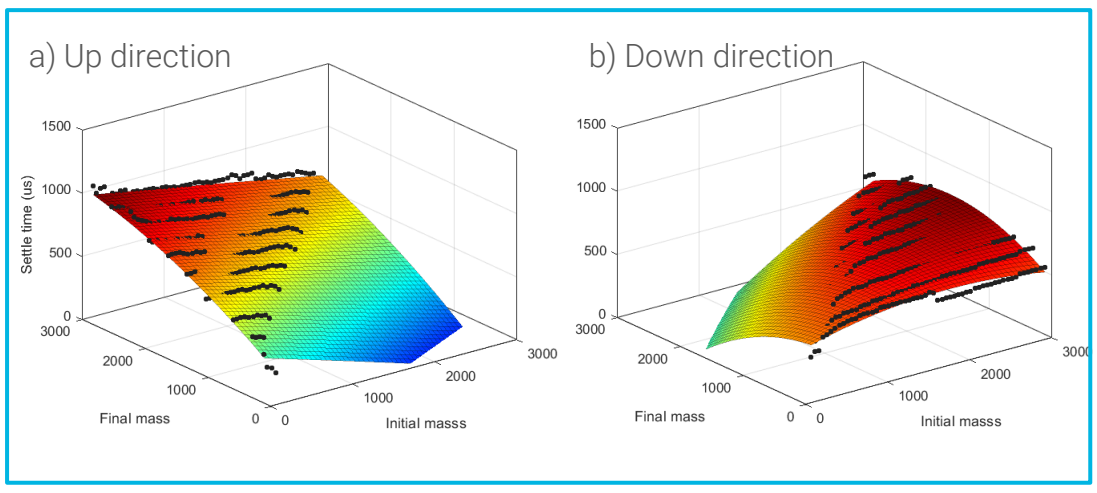

Figure 5. 3D plots of [$(m/z)_{initial}$–$(m/z)_{target}$–Time] data. Poly22 surface fits are shown for each plot.

The settling time data is further separated into up and down directions to account for asymmetry in hardware. Each set of data points are best fitted into a second order polynomial equation in the following format, where "P" terms are coefficients obtained from fitting.

$$\text{Time (us)} = P00 + [P10 * (m/z)_{initial}] + [P01 * (m/z)_{final}] + [P20 * (m/z)_{initial}^{2}] + [P11 * (m/z)_{initial} * (m/z)_{final}] + [P02 * (m/z)_{final}^{2}]$$

Fragmentor delay

A separate set of measurements were performed by changing fragmentor voltage only. The settling times as function of delta fragmentor voltage are plotted in Figure 6a for each tune ion. In general, larger voltage change and ions with lower *m/z* requires longer settling time.

Figure 6b shows the settling time as function of ion *m/z* for both positive and negative ions. The settling time is affected by both the electronics settling (fragmentor voltage) and the ion transition into detector. The interaction between ions and gas flow inside the ion guide tends to slow down low *m/z* ions.

Both sets of data are fitted into second order polynomial correlation. The larger predicted settling time will be applied as inter-measurement delay.

a) Settling time as function of delta fragmentor voltage.

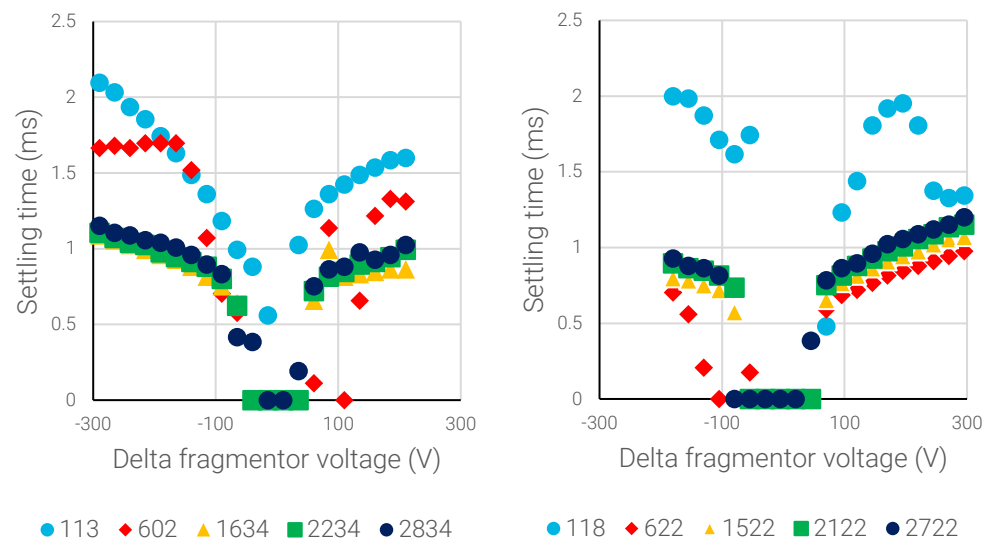

b) Settling time as function of *m/z*.

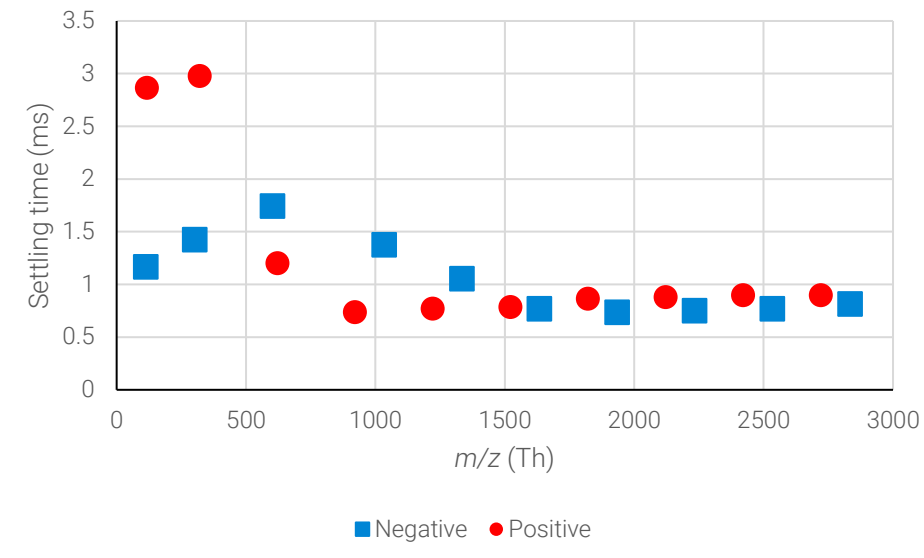

Figure 6. a) Ion abundance settling time in as function of delta fragmentor voltage. b). Settling time as function of *m/z* for both positive and negative ions.

Results and Discussion

Detector gain delay

Detector gain factor can be used for simultaneous detection of ions with drastically different intensity. Changing detector gain factor is achieved by changing voltage applied on electron multiplier (EMV). Figure 7 shows the correlation between settling time and the delta EMV for *m/z* 602. The settling time is fitted against the delta EMV into second order polynomial correlation.

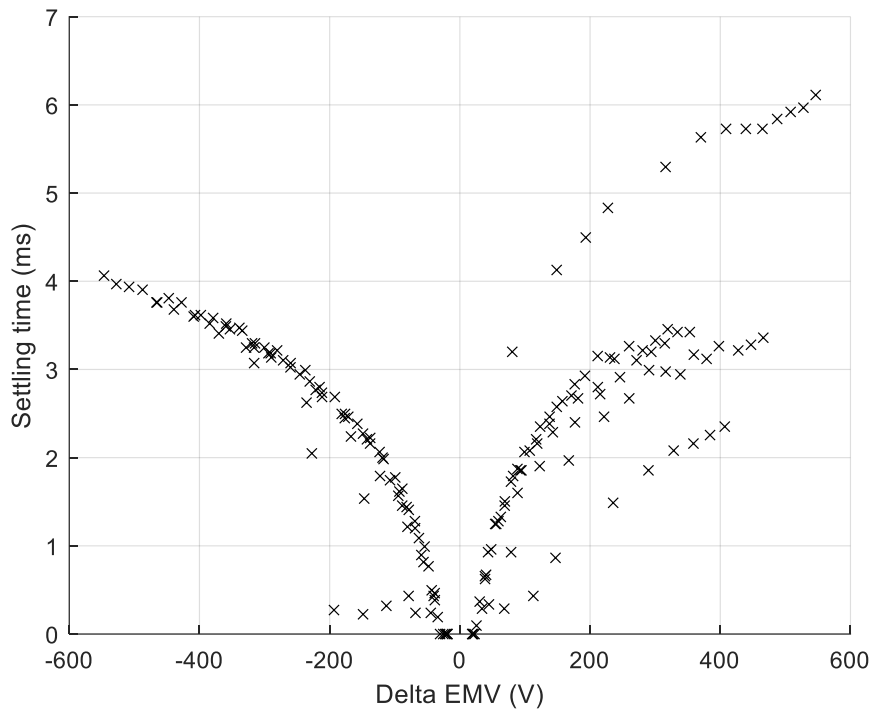

Figure 7. Ion abundance (*m/z* 602) settling time in ms as function of delta EMV voltage.

Polarity switching delay

Ion abundance data after ion polarity switching are shown in Figure 8. Settling time appear to be independent with *m/z* and ion polarity. Fixed delay time can be applied.

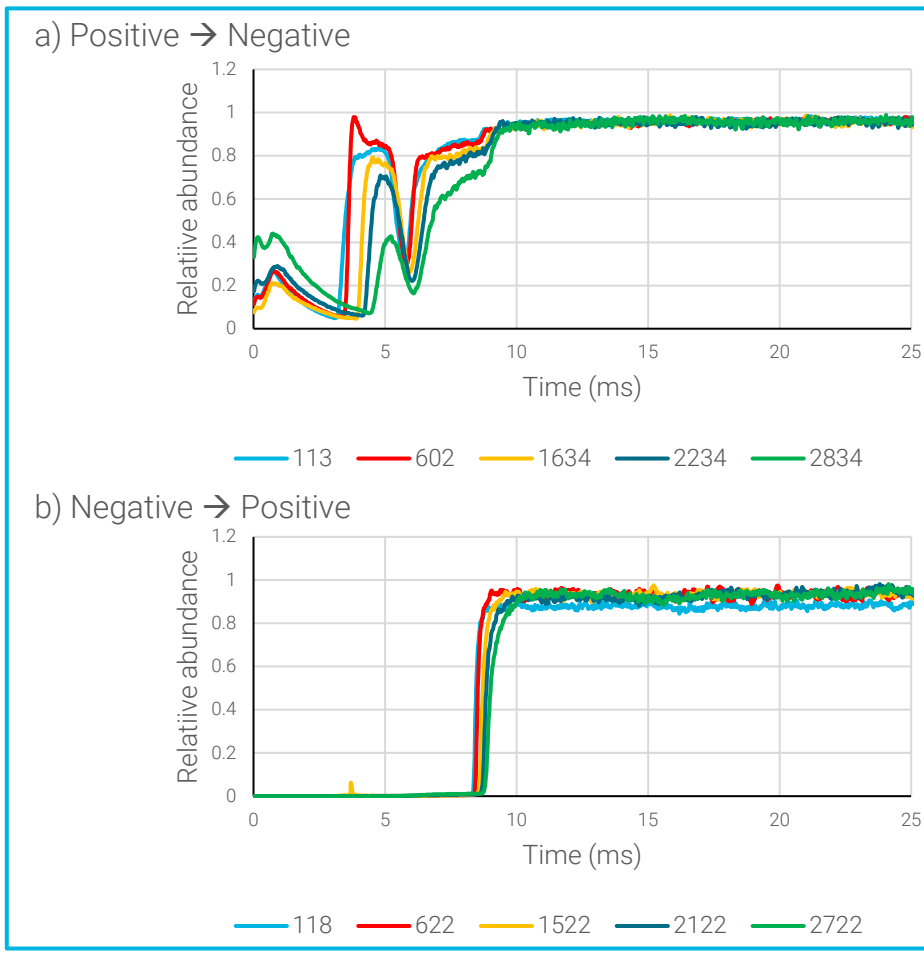

Figure 8. Ion abundance settling after polarity switching from a) positive to negative and b) negative to positive.

Conclusions

Inter-measurement delay time can be predicted from acquisition parameters based on coefficients derived from experimental data.

Instrument control firmware (embedded software) calculate delay time based on multiple sets of coefficients and changes in acquisition parameters.

- Change of ion mass-to-charge ratio
  - For *m/z* going upwards
  - For *m/z* going downwards
  - For no change in *m/z*
- Change of fragmentor voltage
  - Delta fragmentor voltage
  - Final *m/z*
- Change of detector gain factor (delta EMV)
- Change of ion polarity

Acquisition efficiency can be optimized by adjusting the method to minimize total delay time within each cycle.

Based on the impact on ion settling time, acquisition within each cycle should be sorted following the order of ion polarity, detector gain factor, fragmentor voltage and *m/z*.

Coefficients can be further tailored to each instrument.

Empirical coefficients can be shared within instruments with the same hardware design. However, instrument specific coefficients could further reduce delay time without sacrificing analytical performance of the instrument.

References

Zekavat B, Pollum LL, Wang H, Nguyen H, Bui H, Tichy SE. ASMS Annual Conference 2018.

https://www.agilent.com/en/promotions/asms

DE-006642

Published in USA, May 15, 2025

Agilent
Trusted Answers